

# Open system dynamics in linear-time beyond the wide-band limit

Y. Pavlyukh<sup>1</sup> and R. Tuovinen<sup>2</sup>

<sup>1</sup>*Institute of Theoretical Physics, Faculty of Fundamental Problems of Technology,  
Wrocław University of Science and Technology, 50-370 Wrocław, Poland\**

<sup>2</sup>*Department of Physics, Nanoscience Center, P.O. Box 35, 40014 University of Jyväskylä, Finland<sup>†</sup>*

Nonequilibrium heat transport in quantum systems coupled to wide-band embeddings provides a striking example of the limitations of the generalized Kadanoff-Baym ansatz (GKBA), while solving the full two-time Kadanoff-Baym equations remains computationally prohibitive. To address this challenge, we propose an iterated solution to the reconstruction problem, resulting in a time-linear evolution scheme involving 14 correlators for systems with narrow-band embeddings. This approach eliminates GKBA-related artifacts and resolves convergence issues associated with the wide-band limit. Furthermore, it enables the calculation of energy- and time-resolved currents, facilitating the modeling of heat flows in quantum systems and energy- and time-resolved photoemission experiments, all at significantly reduced computational cost.

*Introduction.*—Thermodynamics predates electrodynamics, especially when considering foundational theories. Because transport of charge plays such a fundamental technological role, the phenomenon is well understood and formalized down to quantum, topological and nonequilibrium levels [1–3]. On the other hand, thermal management in electronics and, in perspective, heat control in quantum processors, nanoscale energy harvesting, quantum heat engines require similar understanding of the transport of energy [4–6]. This is closely related (Wiedemann-Franz law) but much less understood phenomenon: Unlike electron current, heat flux is difficult to measure on the nanoscale [7]. Since multiple carriers and mechanisms are involved, it is difficult to formalize [8, 9].

Further indications that heat flow is in many ways fundamentally different from charge flow arise from the consideration of electron transport within the formalism of nonequilibrium Green’s functions (NEGF) [10–12]. In the time-linear formulation [13] derived utilizing the generalized Kadanoff-Baym ansatz (GKBA), the open system dynamics is described in terms of an “embedding correlator” from which the time-dependent current can be calculated using the Meir-Wingreen formula. The so-called wide-band limit approximation (WBLA) is a crucial ingredient of the theory allowing one to close the equations of motion. However, due to diverging energy integrals in the wide-band limit approximation, a simple generalization of the formalism towards the computation of heat currents represents a conceptual problem.

Besides this mathematical aspect, the validity of WBLA relies on the uniformity of the density of electronic states of the leads, which should be verified for each scenario [14, 15]. In addition to transport experiments, the concept of embedding self-energy arises in the treatment of any open system, for instance, in the description of electron photoemission [16, 17], where energy-selective detection of particles requires departing from WBLA.

Therefore in this work, we lay down a time-linear scheme for open quantum systems with Lorentzian tunneling rates [18]

$$\Gamma_{\alpha,ij}(\omega) = \sum_k T_{ik\alpha} T_{k\alpha j} \delta(E_{k\alpha} - \omega) = \frac{\gamma_{\alpha,ij} \Omega_\alpha^2}{(\omega - \epsilon_\alpha)^2 + \Omega_\alpha^2}, \quad (1)$$

where  $\epsilon_\alpha$  and  $\Omega_\alpha$  is the energy centroid and bandwidth, respectively, whereas  $\gamma_\alpha$  is the level-width matrix depending on the coupling  $T_{ik\alpha}$  between the state  $i$  of central region to the state  $k$  of the lead  $\alpha$  with energy  $E_{k\alpha}$ .

*Density and currents.*— We focus here on the electronic transport mechanism and therefore start from the Kadanoff-Baym equation (KBE) for the electronic Green’s function (GF) on the Keldysh contour  $C$ ,

$$\left[ i \frac{d}{dz} - h(z) \right] G(z, z') = \delta(z, z') + \int_C d\bar{z} [\Sigma_c(z, \bar{z}) + \Sigma_{\text{em}}(z, \bar{z})] G(\bar{z}, z'), \quad (2)$$

where  $h$  is the one-electron mean-field (MF) Hamiltonian,  $\Sigma_c$  is the correlation self-energy, and  $\Sigma_{\text{em}} = \sum_\alpha \Sigma_\alpha$  is the embedding self-energy (SE) due to leads—they are matrices in a suitably chosen basis. For simplicity of presentation, we include only the latter part into consideration noting that it is possible to incorporate electronic and electron-boson correlations as demonstrated in Ref. [13]. The electronic GF gives access to different physical observables including currents

$$J_\alpha^\nu(t) = \frac{d}{dt} \left\langle \sum_k E_{k\alpha}^v \hat{c}_{k\alpha}^\dagger \hat{c}_{k\alpha} \right\rangle = 2 \text{Re Tr} [I_\alpha^\nu(t)]. \quad (3)$$

Here,  $\hat{c}_{k\alpha}$  operator is associated with noninteracting electrons of the leads, and charge ( $\nu = 0$ ) and energy ( $\nu = 1$ ) currents are expressed in terms of the collision integrals

$$I_\alpha^\nu(t) = \int dt' [\Sigma_\alpha^{\nu,<}(t, t') G^A(t', t) + \Sigma_\alpha^{\nu,R}(t, t') G^<(t', t)]. \quad (4)$$

The charge part was derived by Jauho, Meir and Wingreen [1, 19], and later it was generalized to energy currents by several authors (see Ref. [20] and references therein). For brevity of notations we denote the ordinary self-energy as  $\Sigma_\alpha^0 = \Sigma_\alpha$ , and  $\Sigma_\alpha^1$  entering the expression for the energy current will be defined below. In Eq. (3), GFs and SEs are functions of real times, therefore lesser (<), retarded (R), and advanced (A) components appear by virtue of the Langreth rules [10].

Dealing with the lesser GF component in Eq. (4) is a fundamental problem of the NEGF formalism. Splitting any lesser

correlator into terms of retarded and advanced types

$$F^<(t, t') = \theta(t - t')F_R^<(t, t') - \theta(t' - t)F_A^<(t, t'), \quad (5)$$

where  $\theta(\tau)$  is the Heaviside step function,  $G_A^<$  in Eq. (4) fulfills the celebrated exact reconstruction equation [21]:

$$G_A^<(t, t') = -\rho(t)G^A(t, t') - \int dy dx \{G^R(t, y)\Sigma^<(y, x) + G_R^<(t, y)\Sigma^A(y, x)\}\theta(x - t)G^A(x, t'), \quad (6)$$

with  $x, y$  denoting intermediate times. Over years, only the first part of this equation — what is conventionally known as GKBA — was considered leading to the impressive progress in the treatment of correlated electronic [22, 23], bosonic [24, 25], and open [13, 26] systems. The key to this success was the ability to reformulate the complicated integro-differential equation (2) into a system of ordinary differential equations (ODEs), which can conveniently be propagated with linear scaling in physical time. However, some limitations of the time-linear scheme have been identified such as unphysical electron densities in electronic [27] and electron-boson systems [28], as well as currents in open systems [29, 30].

In a series of works [29–31], Kalvová, Špička, Velický, and Lipavský demonstrated dramatic improvements in the treatment of electronic transport, by approximately including correction terms in Eq. (6). Their method involves the so-called Markovian [30] or mirrored ( $m$ ) [32] GKBA  $G_R^<(x, z) = -\rho(x)G^R(x, z)$  in the rhs of Eq. (6). However, their hybrid scheme—combining the conventional GKBA as a leading term with  $m$ GKBA in the corrections—relies on further approximations to evaluate the complex collision terms.

We demonstrate here that it is possible to deal with the reconstruction equation in a pure ODE way (akin of Ref. [13] for the wide-band limit) while retaining time-linear scaling and thus achieving high numerical efficiency. Crucially, no additional approximations are introduced beyond the use of GKBA  $G_R^<(x, z) = -G^R(x, z)\rho(z)$  in the correction term of Eq. (6), hence we term our method the iterated generalized Kadanoff-Baym ansatz ( $i$ GKBA).

In the considered scenario, in addition to time-dependent MF  $h(t)$ , the dynamics is driven by voltages  $V_\alpha(t)$  applied to the leads, and by the ramp function  $s_\alpha(t)$  associated with tunneling matrix elements, i.e.,  $T_{ik\alpha} \rightarrow T_{ik\alpha}s_\alpha(t)$ . This allows us to build a correlated initial state by the adiabatic switching procedure, and for the lead  $\alpha$ , results in the time-prefactor

$$s_\alpha(t)e^{-i\phi_\alpha(t, t')}s_\alpha(t') = s_\alpha(t)\sigma_\alpha(t, t') = s_\alpha(t)u_\alpha(t, t')s_\alpha(t'), \quad (7)$$

where  $\phi_\alpha(t, t') \equiv \int_{t'}^t dx V_\alpha(x)$  is the accumulated phase due to the applied voltage. The SE components read [10]:

$$\Sigma_\alpha^{v,R}(t, t') = -is_\alpha(t)\sigma_\alpha(t, t')\mathcal{F}[\omega^\nu \Gamma_\alpha(\omega)](t - t')\theta(t - t'), \quad (8a)$$

$$\Sigma_\alpha^{v,<}(t, t') = is_\alpha(t)\sigma_\alpha(t, t')\mathcal{F}[\omega^\nu f_\alpha(\omega)\Gamma_\alpha(\omega)](t - t'), \quad (8b)$$

where  $\mathcal{F}[a](\tau) = \int \frac{d\omega}{2\pi} e^{-i\omega\tau} a(\omega)$  is the Fourier transform and  $f_\alpha(\omega)$  is the Fermi-Dirac (FD) distribution function (for inverse temperature  $\beta_\alpha$  and chemical potential  $\mu_\alpha$ ), which we write using a suitable pole expansion [33]

$$f_\alpha(\omega) = \frac{1}{e^{\beta_\alpha(\omega - \mu_\alpha)} + 1} = \frac{1}{2} - \sum_{\ell \geq 1} \eta_\ell \left[ \frac{1}{\beta_\alpha(\omega - \mu_\alpha) + i\zeta_\ell} + \frac{1}{\beta_\alpha(\omega - \mu_\alpha) - i\zeta_\ell} \right], \quad \text{with } \text{Re } \zeta_\ell > 0. \quad (9)$$

Performing the Fourier transforms (8) by closing the integration contour in the complex lower, upper half-plane we obtain for  $\Sigma_\alpha^R(t, x) = s_\alpha(t)\bar{\Sigma}_\alpha^R(t, x)$ ,  $\Sigma_\alpha^A(x, t) = \bar{\Sigma}_\alpha^A(x, t)s_\beta(t)$ , respectively:

$$\bar{\Sigma}_\alpha^R(t, x) = -\frac{i}{2}\Omega_\alpha \gamma_\alpha u_\alpha(t, x)s_\alpha(x)e^{-i\bar{\epsilon}_\alpha(t-x)}\theta(t - x), \quad (10a)$$

$$\bar{\Sigma}_\beta^A(x, t) = \frac{i}{2}\Omega_\beta \gamma_\beta e^{i\bar{\epsilon}_\beta^*(t-x)}s_\beta(x)u_\beta(x, t)\theta(t - x). \quad (10b)$$

where we introduced  $\bar{\epsilon}_\alpha = \epsilon_\alpha - i\Omega_\alpha$  and used  $x$  to denote intermediate times in convolution integrals, and Greek subscripts to enumerate leads ( $1 \leq \alpha, \beta \leq N_{\text{leads}}$ ).

For the lesser component of embedding SE [ $\Sigma_{R,\alpha}^<(t, x) = s_\alpha(t)\bar{\Sigma}_{R,\alpha}^<(t, x)$  and  $\Sigma_{A,\beta}^<(x, t) = \bar{\Sigma}_{A,\beta}^<(x, t)s_\beta(t)$ ] we analogously have:

$$\begin{aligned} \bar{\Sigma}_{R,\alpha}^<(t, x) &= iu_\alpha(t, x) \left\{ \gamma_\alpha \frac{\Omega_\alpha}{2} f_\alpha(\epsilon_\alpha - i\Omega_\alpha) e^{-i\bar{\epsilon}_\alpha(t-x)} + i \sum_{\ell \geq 1} \frac{\eta_\ell}{\beta_\alpha} \Gamma_\alpha \left( \mu_\alpha - i\frac{\zeta_\ell}{\beta_\alpha} \right) e^{-i\left(\mu_\alpha - i\frac{\zeta_\ell}{\beta_\alpha}\right)(t-x)} \right\} s_\alpha(x) \\ &= u_\alpha(t, x)s_\alpha(x) \sum_{\ell \geq 0} \bar{\eta}_{\alpha\ell} e^{-i\bar{\mu}_{\alpha\ell}(t-x)} = \sum_{\ell \geq 0} \bar{\eta}_{\alpha\ell} \bar{\Sigma}_{R,\alpha\ell}^<(t, x). \end{aligned} \quad (11)$$

where the expansion coefficients  $\bar{\eta}_{\alpha\ell}$  and the exponents  $\bar{\mu}_{\alpha\ell}$  are given by

$$\bar{\eta}_{\alpha\ell} = \begin{cases} i\frac{\gamma_\alpha}{2}\Omega_\alpha f_\alpha(\epsilon_\alpha - i\Omega_\alpha) & \ell = 0, \\ -\frac{\eta_\ell}{\beta_\alpha} \Gamma_\alpha \left( \mu_\alpha - i\frac{\zeta_\ell}{\beta_\alpha} \right) & \ell \geq 1; \end{cases} \quad \bar{\mu}_{\alpha\ell} = \begin{cases} \epsilon_\alpha - i\Omega_\alpha & \ell = 0, \\ \mu_\alpha - i\frac{\zeta_\ell}{\beta_\alpha} & \ell \geq 1. \end{cases} \quad (12)$$

Analogously, for the lesser SE of advanced type (remember the incorporated minus sign, cf. Eq. 5) we obtain:

$$\bar{\Sigma}_{A,\beta}^<(x, t) = u_\beta(x, t)s_\beta(x) \sum_{\ell \geq 0} \bar{\eta}_{\beta\ell}^* e^{i\bar{\mu}_{\beta\ell}^*(t-x)} = \sum_{\ell \geq 0} \bar{\eta}_{\beta\ell}^* \bar{\Sigma}_{A,\beta\ell}^<(x, t). \quad (13)$$

Inserting the embedding SEs (10a) and (11) into Eq. (4) yields four contributions to the collision integral. Defining

$$[af \cdot b](t, t') = \int dx a(t, x)f(x)b(x, t'), \quad (14a)$$

$$[af \cdot b]_A(t, t') = \theta(t' - t)[af \cdot b](t, t') \quad (14b)$$

to simplify notations, the first term in the collision integral (6) can be expressed in terms of

$$D_{\alpha\ell}^c(t) = [\bar{\Sigma}_{R,\alpha\ell}^< \cdot G^A](t, t). \quad (15)$$

Second collision term in combination with the first term of the reconstruction equation leads to

$$D_{\alpha}^d(t) = [\bar{\Sigma}_{\alpha}^R \rho \cdot G^A](t, t). \quad (16)$$

Finally, the correction terms in Eq. (6) give rise to

$$\mathcal{A}_{\alpha\beta}^a(t) = [\bar{\Sigma}_{\alpha}^R \cdot [G^R \cdot \Sigma_{\beta}^<]_A \cdot G^A](t, t), \quad (17a)$$

$$\mathcal{A}_{\alpha\beta}^b(t) = [\bar{\Sigma}_{\alpha}^R \cdot [G^R \rho \cdot \Sigma_{\beta}^A]_A \cdot G^A](t, t). \quad (17b)$$

In the hybrid scheme  $iGKBA(h)$ , which arises from using  $mGKBA$  in the correction part of Eq. (6),  $\rho$  in Eq. (17b) is positioned after  $G^R$ . This slightly modifies the equations of motion, without any pronounced physical effect, as numerically demonstrated below.

Due to the simple form of the embedding self-energy, it can be shown that the correlators satisfy a system of coupled ODEs. Consider for instance the time-derivative of  $\mathcal{A}^a(t)$ :

$$\begin{aligned} i \frac{d}{dt} \mathcal{A}_{\alpha\beta}^a(t) &= \mathcal{A}_{\alpha\beta}^a(t) [V_{\alpha}(t) + \epsilon_{\alpha} - i\Omega_{\alpha} - h^{\dagger}(t)] \\ &\quad - s_{\beta}(t) [\bar{\Sigma}_{\alpha}^R \cdot [G^R \cdot \bar{\Sigma}_{\beta}^<]_A](t) \\ &\quad - \sum_{\gamma} s_{\gamma}(t) [\bar{\Sigma}_{\alpha}^R \cdot [G^R \cdot \Sigma_{\beta}^<]_A \cdot G^A \cdot \bar{\Sigma}_{\gamma}^A](t). \end{aligned} \quad (18)$$

The first oscillatory term originates from the derivative of  $u_{\alpha}$ , the exponent in  $\bar{\Sigma}_{\alpha}^R$  (10a), and from the mean-field part of the EOM for  $G^A(y, t)$ . The simpler second term results from the differentiation of the  $\theta$ -function in  $\bar{\Sigma}_{\alpha}^R$  and  $G^A$  yielding a  $\delta$ -function contribution, which can easily be integrated over. Finally, the third term results from the correlation term in the EOM for  $G^A(y, t)$ . It leads to a more complicated correlator. The process of derivation is visualized in Fig. 1, where it is shown that  $\mathcal{A}_{\alpha\beta}^a$  gives rise to  $\mathcal{B}_{\alpha\beta\ell}^a$  and  $\mathcal{C}_{\alpha\beta\gamma}^a$  correlators. Other correlators are treated similarly leading to in total 14 functions defined in Fig. 1. The corresponding EOMs follow a structure analogous to Eq. (18); while straightforward, they are too lengthy to present here (see Supplemental Material [34]). The overall computational scaling is  $\mathcal{O}(N_{\text{sys}}^3 N_{\text{leads}}^2 (2N_{\text{leads}} + 4N_p))$ .

The collision integral (4) can be written as:

$$\begin{aligned} I_{\alpha}(t) &= [\Sigma_{\alpha}^< \cdot G^A + \Sigma_{\alpha}^R \cdot G^<](t, t) \\ &= s_{\alpha}(t) \left[ \sum_{\ell \geq 0} \bar{\eta}_{\alpha\ell} [\bar{\Sigma}_{\alpha\ell}^< \cdot G^A] - [\bar{\Sigma}_{\alpha}^R \cdot G_A^<] \right](t, t) \end{aligned} \quad (19)$$

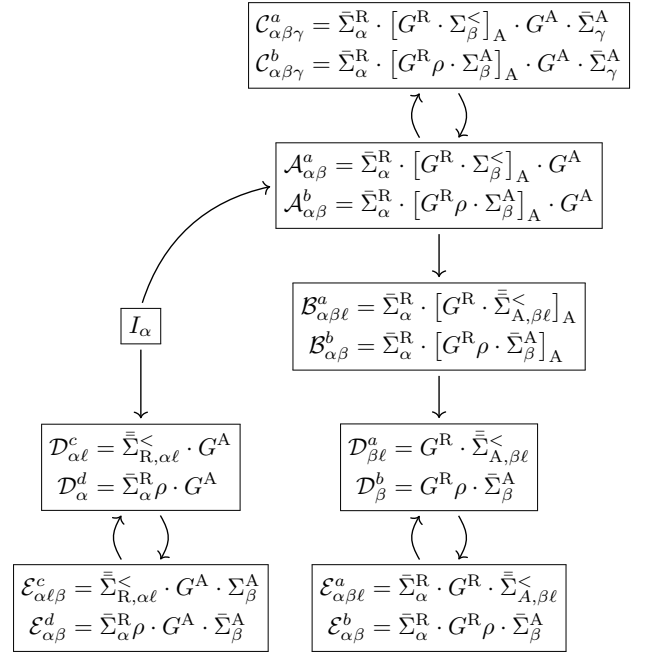


FIG. 1. Derivation of EOMs for the  $iGKBA$  correlators.

$$= s_{\alpha}(t) \left\{ \sum_{\ell \geq 0} \bar{\eta}_{\alpha\ell} D_{\alpha\ell}^c(t) + D_{\alpha}^d(t) + \sum_{\beta} [\mathcal{A}_{\alpha\beta}^a - \mathcal{A}_{\alpha\beta}^b](t) \right\}.$$

To get the last equation, we substituted for  $G_A^<$  the reconstruction equation (6) and used explicit definitions of  $\mathcal{A}$  (17) and  $\mathcal{D}$  (15, 16) correlators. Knowing  $I_{\alpha}(t)$ , density matrix can be propagated  $\frac{d}{dt} \rho(t) = -(ih(t)\rho(t) + \sum_{\alpha} I_{\alpha}(t)) + h.c.$ , and charge current can be computed according to Eq. (3).

For the energy current,  $I_{\alpha}^{(1)}(t)$  is needed. This collision integral is computed similarly to Eq. (19),  $I_{\alpha}^{(1)}(t) = [\Sigma_{\alpha}^{1,<} \cdot G^A + \Sigma_{\alpha}^{1,R} \cdot G^<](t, t)$ . Starting from the Fourier representations, the relations between  $\nu = 0$  and  $\nu = 1$  self-energies follow  $\bar{\Sigma}_{\alpha}^{1,R} = \bar{\epsilon}_{\alpha} \bar{\Sigma}_{\alpha}^R$ ,  $\bar{\Sigma}_{R,\alpha}^{1,<} = \sum_{\ell \geq 0} \bar{\mu}_{\alpha\ell} \bar{\eta}_{\alpha\ell} \bar{\Sigma}_{R,\alpha\ell}^<$  leading to

$$\begin{aligned} I_{\alpha}^{(1)}(t) &= s_{\alpha}(t) \left\{ \sum_{\ell \geq 0} \bar{\mu}_{\alpha\ell} \bar{\eta}_{\alpha\ell} D_{\alpha\ell}^c(t) + \bar{\epsilon}_{\alpha} D_{\alpha}^d(t) \right. \\ &\quad \left. + \bar{\epsilon}_{\alpha} \sum_{\beta} [\mathcal{A}_{\alpha\beta}^a - \mathcal{A}_{\alpha\beta}^b](t) \right\}. \end{aligned} \quad (20)$$

Eqs. (19 and 20), together with EOMs for the constituent  $\mathcal{A}$ ,  $\mathcal{B}$ ,  $\mathcal{C}$ ,  $\mathcal{D}$ , and  $\mathcal{E}$  correlators represent the main result of this work.

*Numerical demonstration.*— A stringent test for open system calculations with narrow-band leads involves a scenario where a central system is connected to two leads with aligned chemical potentials and identical temperatures. From the Landauer–Büttiker (LB) formula [10]

$$\begin{aligned} J_{\alpha}^{(0)} &= \int \frac{d\omega}{2\pi} \sum_{\beta} (f_{\alpha}(\omega - V_{\alpha}) - f_{\beta}(\omega - V_{\beta})) \\ &\quad \times \text{Tr} [\Gamma_{\alpha}(\omega - V_{\alpha}) G^R(\omega) \Gamma_{\beta}(\omega - V_{\beta}) G^A(\omega)] \end{aligned} \quad (21)$$

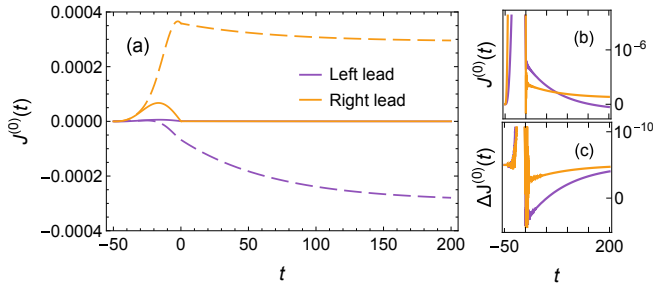


FIG. 2. (a) Electric currents computed within GKBA (dashed) and  $i$ GKBA (full) methods. (b) Deviation of the  $i$ GKBA results from zero. (c) Difference between the  $i$ GKBA(h) and  $i$ GKBA currents. High accuracy is ensured by the use of an adaptive step-size ODE solver.

such a system should exhibit no steady-state currents, even when the spectral densities  $\Gamma_\alpha$  and  $\Gamma_\beta$  are centered at different energies [35]. In our first setup, a central site with energy  $\epsilon_0 = -3$  is connected to two leads with  $\mu_1 = \mu_2 = 0$ , inverse temperatures  $\beta_1 = \beta_2 = 30$ , and level widths  $\gamma_1 = \gamma_2 = 0.5$ . The initial state is prepared by adiabatically turning on the hopping to the leads on the time interval  $[t_i, 0]$ ,  $t_i = -50$  using the ramp functions  $s_\alpha(t) = \cos(\pi/2 \cdot t/t_i)^2 \theta(-t) + \theta(t)$ . For  $t > 0$ , the system evolves without any applied voltages. In Fig. 2, we compare charge currents computed using different methods for the leads centered at  $\epsilon_1 = -10$  and  $\epsilon_2 = 10$ .

The standard GKBA approximation obtained by neglecting the  $\mathcal{A}$  correlators in Eq. (19), yields physically incorrect results, as indicated by the dashed lines. Persistent currents flow between the leads despite the absence of a driving force. Notably, there is no charge accumulation on the central site, as the sum of the currents remains zero. The  $i$ GKBA and  $i$ GKBA(h) theories provide a much more accurate physical description: the steady-state currents remain around  $10^{-6}$  (panel b), with their difference being even smaller,  $\sim 10^{-10}$  (panel c).

Following this sanity check, we proceed to investigate more complex, bias-driven scenarios. We consider a resonant-level system described Kara Slimane *et al.* [20]. In this *noninteracting* model a central site with energy  $\epsilon_0(t) = 0.5$  is connected to two leads ( $\gamma_{1,2} = 0.5$ ) with different temperatures and chemical potentials:  $\beta_1 = 1$ ,  $\mu_1 = 0.5$  and  $\beta_2 = 10$ ,  $\mu_2 = -0.5$ . The initial state is prepared by following the same adiabatic protocol. At  $t = 0$ , time-dependent bias voltages are applied  $V_\alpha(t) = -2.5[1 + \exp(-25t)]^{-1}$ . In Fig. 3 we focus on the heat currents defined as

$$J_\alpha^H(t) = J_\alpha^{(1)}(t) - \mu_\alpha J_\alpha^{(0)}(t). \quad (22)$$

Here, the GKBA (dashed line) exhibits a notable artifact: a significant negative shift in the heat current, attributable solely to inaccuracies in the energy current  $J^{(1)}$ , as all considered methods accurately predict the occupation of the central site  $\rho(t)$  and the charge currents  $J^{(0)}(t)$  [34]. Fig. 3 demonstrates that  $i$ GKBA results converge toward the exact analytic WBLA solution as the spectral broadening  $\Omega$  increases. Note that calculations for higher values of  $\beta_\alpha$  and  $\epsilon_\alpha - i\Omega_\alpha$  require more

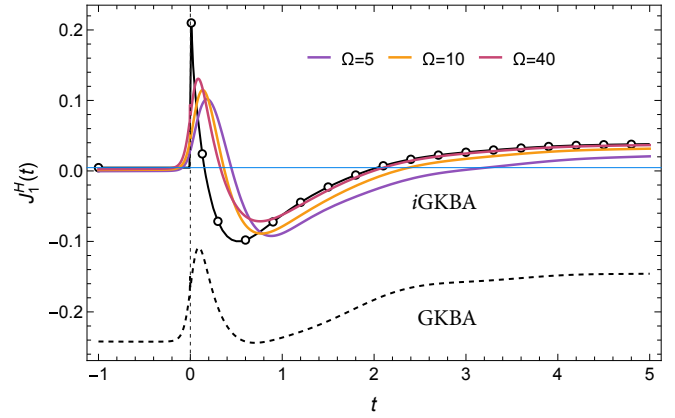


FIG. 3. Heat currents of a resonant level system. Dots represent exact analytic results for wide-band leads.  $i$ GKBA calculations for three different  $\Omega$  values show substantial improvement over the GKBA result ( $\Omega = 40$ , dashed line). Blue line denotes a stationary LB value.

terms ( $N_p$ ) in the partial fraction expansion (9) of  $f_\alpha(\bar{\epsilon}_\alpha)$ .

Our approach is not restricted to Lorentzian spectral densities. By coupling the system to multiple leads, various shapes of the tunneling rates can be achieved, enabling energy- and time-resolved current calculations, Fig. 4. As an example, we extend the resonant-level model by replacing the left lead with 21 narrow sub-leads ( $\Omega_{1j} = 1$ ,  $\beta_{1j} = 1$  and  $\gamma_{1j} = 0.16$ ) centered at  $\epsilon_j = j$  with  $-10 \leq j \leq 10$ . The right lead parameters remain  $\Omega_2 = 15$ ,  $\beta_2 = 10$  and  $\gamma_2 = 0.5$ . Simulations under the same

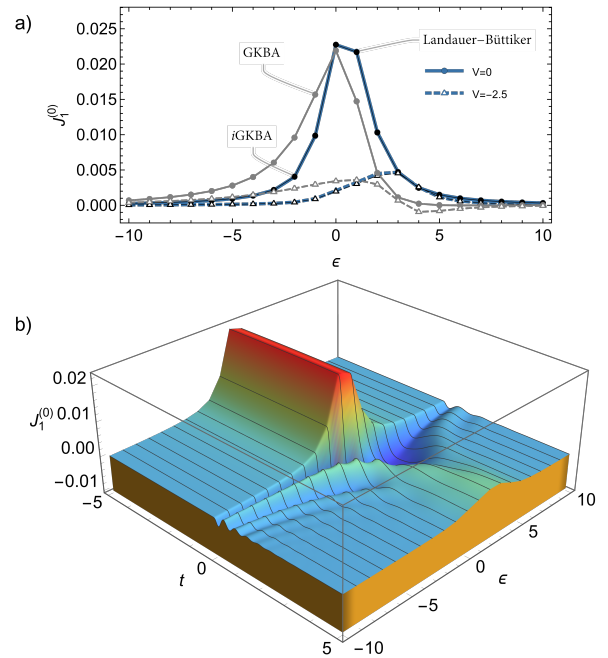


FIG. 4. Charge currents of a resonant-level system. Top: steady state currents before and after the voltage activation from the LB equation (21) showing superiority of  $i$ GKBA over GKBA. Bottom:  $i$ GKBA energy- and time-resolved currents.



excitation protocol illustrate the distinct spectral distribution of currents in the stationary states before and after bias activation, where *i*GKBA agrees perfectly with the LB prediction, along with a complex transient evolution.

*Conclusion.*— The achieved progress is therefore two-fold: i) We developed a time-linear nonequilibrium theory for the treatment of open systems coupled to *narrow-band leads*. ii) As conventional GKBA is insufficient for this scenario, we put forward an *i*GKBA+ODE scheme corresponding to the first iteration of the reconstruction equation. Moreover, we resolved a debated issue about the choice of approximation for  $G^{A/R}(t-t')$  in GKBA [15, 36–41]. For open systems, we demonstrate that such approximations are unnecessary and can be fully incorporated into our formalism. This framework paves the way for exploring higher-order iterative reconstructions and potential extensions to correlated electronic and bosonic systems. We anticipate applications in studying nonequilibrium heat flows [5, 6, 42, 43] and modeling energy- and time-resolved photoemission experiments [44]—scenarios beyond the reach of conventional GKBA approaches.

#### ACKNOWLEDGEMENT

R.T. acknowledges the EffQSim project funded by the Jane and Aatos Erkkö Foundation.

\* [yaroslav.pavlyukh@pwr.edu.pl](mailto:yaroslav.pavlyukh@pwr.edu.pl)

† [riku.m.s.tuovinen@jyu.fi](mailto:riku.m.s.tuovinen@jyu.fi)

- [1] Y. Meir and N. S. Wingreen, Landauer formula for the current through an interacting electron region, *Phys. Rev. Lett.* **68**, 2512 (1992).
- [2] M. N. Chernodub, Y. Ferreiros, A. G. Grushin, K. Landsteiner, and M. A. Vozmediano, Thermal transport, geometry, and anomalies, *Phys. Rep.* **977**, 1 (2022).
- [3] S. Kurth, G. Stefanucci, C.-O. Almbladh, A. Rubio, and E. K. U. Gross, Time-dependent quantum transport: A practical scheme using density functional theory, *Phys. Rev. B* **72**, 035308 (2005).
- [4] Y. Dubi and M. Di Ventra, *Colloquium*: Heat flow and thermoelectricity in atomic and molecular junctions, *Rev. Mod. Phys.* **83**, 131 (2011).
- [5] J. P. Pekola and B. Karimi, *Colloquium*: Quantum heat transport in condensed matter systems, *Rev. Mod. Phys.* **93**, 041001 (2021).
- [6] L. Arrachea, Energy dynamics, heat production and heat-work conversion with qubits: toward the development of quantum machines, *Rep. Prog. Phys.* **86**, 036501 (2023).
- [7] P. Reddy, S.-Y. Jang, R. A. Segalman, and A. Majumdar, Thermoelectricity in Molecular Junctions, *Science* **315**, 1568 (2007).
- [8] J. M. Luttinger, Theory of Thermal Transport Coefficients, *Phys. Rev.* **135**, A1505 (1964).
- [9] M. Galperin, A. Nitzan, and M. A. Ratner, Heat conduction in molecular transport junctions, *Phys. Rev. B* **75**, 155312 (2007).
- [10] G. Stefanucci and R. van Leeuwen, *Nonequilibrium Many-Body Theory of Quantum Systems: A Modern Introduction* (Cambridge University Press, Cambridge, 2013).
- [11] F. Covito, F. G. Eich, R. Tuovinen, M. A. Sentef, and A. Rubio, Transient Charge and Energy Flow in the Wide-Band Limit, *J. Chem. Theory Comput.* **14**, 2495 (2018).
- [12] M. Ridley, N. W. Talarico, D. Karlsson, N. Lo Gullo, and R. Tuovinen, A many-body approach to transport in quantum systems: from the transient regime to the stationary state, *J. Phys. A* **55**, 273001 (2022).
- [13] R. Tuovinen, Y. Pavlyukh, E. Perfetto, and G. Stefanucci, Time-Linear Quantum Transport Simulations with Correlated Nonequilibrium Green’s Functions, *Phys. Rev. Lett.* **130**, 246301 (2023).
- [14] C. J. O. Verzijl, J. S. Seldenthuis, and J. M. Thijssen, Applicability of the wide-band limit in DFT-based molecular transport calculations, *J. Chem. Phys.* **138**, 094102 (2013).
- [15] S. Latini, E. Perfetto, A.-M. Uimonen, R. van Leeuwen, and G. Stefanucci, Charge dynamics in molecular junctions: Nonequilibrium Green’s function approach made fast, *Phys. Rev. B* **89**, 075306 (2014).
- [16] M. Schüler, J. Berakdar, and Y. Pavlyukh, Time-dependent many-body treatment of electron-boson dynamics: Application to plasmon-accompanied photoemission, *Phys. Rev. B* **93**, 054303 (2016).
- [17] E. Perfetto, D. Sangalli, A. Marini, and G. Stefanucci, First-principles approach to excitons in time-resolved and angle-resolved photoemission spectra, *Phys. Rev. B* **94**, 245303 (2016).
- [18] G.-M. Tang and J. Wang, Full-counting statistics of charge and spin transport in the transient regime: A nonequilibrium Green’s function approach, *Phys. Rev. B* **90**, 195422 (2014).
- [19] A.-P. Jauho, N. S. Wingreen, and Y. Meir, Time-dependent transport in interacting and noninteracting resonant-tunneling systems, *Phys. Rev. B* **50**, 5528 (1994).
- [20] A. Kara Slimane, P. Reck, and G. Fleury, Simulating time-dependent thermoelectric transport in quantum systems, *Phys. Rev. B* **101**, 235413 (2020).
- [21] P. Lipavský, V. Špička, and B. Velický, Generalized Kadanoff-Baym ansatz for deriving quantum transport equations, *Phys. Rev. B* **34**, 6933 (1986).
- [22] N. Schlünzen, J.-P. Joost, and M. Bonitz, Achieving the Scaling Limit for Nonequilibrium Green Functions Simulations, *Phys. Rev. Lett.* **124**, 076601 (2020).
- [23] Y. Pavlyukh, E. Perfetto, and G. Stefanucci, Photoinduced dynamics of organic molecules using nonequilibrium Green’s functions with second-Born, *GW*, *T*-matrix, and three-particle correlations, *Phys. Rev. B* **104**, 035124 (2021).
- [24] D. Karlsson, R. van Leeuwen, Y. Pavlyukh, E. Perfetto, and G. Stefanucci, Fast Green’s Function Method for Ultrafast Electron-Boson Dynamics, *Phys. Rev. Lett.* **127**, 036402 (2021).
- [25] Y. Pavlyukh, E. Perfetto, D. Karlsson, R. van Leeuwen, and G. Stefanucci, Time-linear scaling nonequilibrium Green’s function methods for real-time simulations of interacting electrons and bosons. I. Formalism, *Phys. Rev. B* **105**, 125134 (2022).
- [26] R. Tuovinen and Y. Pavlyukh, Electroluminescence Rectification and High Harmonic Generation in Molecular Junctions, *Nano Lett.*, [acs.nanolett.4c02609](https://doi.org/10.1021/acs.nanolett.4c02609) (2024).
- [27] J.-P. Joost, N. Schlünzen, H. Ohldag, M. Bonitz, F. Lackner, and I. Březinová, Dynamically screened ladder approximation: Simultaneous treatment of strong electronic correlations and dynamical screening out of equilibrium, *Phys. Rev. B* **105**, 165155 (2022).
- [28] Y. Pavlyukh, E. Perfetto, D. Karlsson, R. van Leeuwen, and G. Stefanucci, Time-linear scaling nonequilibrium Green’s function method for real-time simulations of interacting electrons and bosons. II. Dynamics of polarons and doublons, *Phys. Rev. B* **105**, 125135 (2022).

- [29] A. Kalvová, B. Velický, and V. Špička, Beyond the Generalized Kadanoff-Baym Ansatz, *Phys. Status Solidi B* **256**, 1800594 (2019).
- [30] A. Kalvová, V. Špička, B. Velický, and P. Lipavský, Dynamical vertex correction to the generalized Kadanoff-Baym Ansatz, *Europhys. Lett.* **141**, 16002 (2023).
- [31] A. Kalvová, V. Špička, B. Velický, and P. Lipavský, Fast corrections to the generalized Kadanoff-Baym ansatz, *Phys. Rev. B* **109**, 134306 (2024).
- [32] G. Stefanucci and E. Perfetto, Semiconductor electron-phonon equations: A rung above Boltzmann in the many-body ladder, *SciPost Physics* **16**, 073 (2024).
- [33] J. Hu, R.-X. Xu, and Y. Yan, Communication: Padé spectrum decomposition of Fermi function and Bose function, *J. Chem. Phys.* **133**, 101106 (2010).
- [34] See Supplemental Material, which includes Ref. [45] for more detailed discussion.
- [35] Note that bias is not incorporated in the definition of the tunneling rate, Eq. (1), and, therefore, must be included in the arguments of  $\Gamma_\alpha$  and  $\Gamma_\beta$  in the Landauer–Büttiker formula.
- [36] N. Schlünzen and M. Bonitz, Nonequilibrium Green Functions Approach to Strongly Correlated Fermions in Lattice Systems, *Contributions to Plasma Physics* **56**, 5 (2016).
- [37] R. Tuovinen, D. Golež, M. Eckstein, and M. A. Sentef, Comparing the generalized Kadanoff-Baym ansatz with the full Kadanoff-Baym equations for an excitonic insulator out of equilibrium, *Phys. Rev. B* **102**, 115157 (2020).
- [38] R. Tuovinen, Electron correlation effects in superconducting nanowires in and out of equilibrium, *New J. Phys.* **23**, 083024 (2021).
- [39] C. Stahl, N. Dasari, J. Li, A. Picano, P. Werner, and M. Eckstein, Memory truncated Kadanoff-Baym equations, *Phys. Rev. B* **105**, 115146 (2022).
- [40] C. Makait, F. B. Fajardo, and M. Bonitz, Time-dependent charged particle stopping in quantum plasmas: testing the G1-G2 scheme for quasi-one-dimensional systems, *Contributions to Plasma Physics* **63**, e202300008 (2023).
- [41] C. C. Reeves, Y. Zhu, C. Yang, and V. Vlček, Unimportance of memory for the time nonlocal components of the Kadanoff-Baym equations, *Phys. Rev. B* **108**, 115152 (2023).
- [42] P. Strasberg, G. Schaller, T. Brandes, and M. Esposito, Quantum and information thermodynamics: A unifying framework based on repeated interactions, *Phys. Rev. X* **7**, 021003 (2017).
- [43] P. Portugal, F. Brange, and C. Flindt, Heat pulses in electron quantum optics, *Phys. Rev. Lett.* **132**, 256301 (2024).
- [44] F. Boschini, M. Zonno, and A. Damascelli, Time-resolved ARPES studies of quantum materials, *Rev. Mod. Phys.* **96**, 015003 (2024).
- [45] Y. Pavlyukh, R. Tuovinen, E. Perfetto, and G. Stefanucci, Cheers: A Linear-Scaling KBE + GKBA Code, *Phys. Status Solidi B* **2023**, 2300504.